Univerza
v Ljubljani

Fakulteta
*za gradbeništvo
in geodezijo*

Jamova 2
1000 Ljubljana, Slovenija
http://www3.fgg.uni-lj.si/

DRUGG – Digitalni repozitorij UL FGG
http://drugg.fgg.uni-lj.si/

Ta članek je avtorjeva zadnja recenzirana različica, kot je bila sprejeta po opravljeni recenziji.

Prosimo, da se pri navajanju sklicujte na bibliografske podatke, kot je navedeno:

University
of Ljubljana

Faculty of
*Civil and Geodetic
Engineering*

Jamova 2
SI – 1000 Ljubljana, Slovenia
http://www3.fgg.uni-lj.si/

DRUGG – The Digital Repository
http://drugg.fgg.uni-lj.si/

This version of the article is author's manuscript as accepted for publishing after the review process.

When citing, please refer to the publisher's bibliographic information as follows:

On Boundary Layer in the Mindlin Plate Model: Levy Plates

Boštjan Brank

University of Ljubljana, Faculty of Civil and Geodetic Engineering
Jamova 2, 1000 Ljubljana, Slovenia, e-mail: bbrank@ikpir.fgg.uni-lj.si

Abstract

This work is related to the bending problem of thick rectangular Levy plates. Series solution for the Mindlin (thick) plate model is obtained and represented as a sum of the Kirchhoff (thin) plate model solution, the "shear terms" and the "boundary layer terms". Hard- and soft-simple supported, hard- and soft-clamped and free boundary conditions are considered. In order to detect plate regions where Kirchhoff model is good enough, and plate regions where Mindlin model should be used, a model error indicator is introduced. Several examples are presented, illustrating the difference between the Mindlin and the Kirchhoff results, the strengths of boundary layers for different boundary conditions, accuracy of several possible model error indicators and dependence of results on plate thickness.

Keywords: Plates, Mindlin plate theory, Kirchhoff plate theory, Levy plates, Boundary layer, Model error indicator

1. Introduction

The bending of plates has been modeled by different theories, which may lead to different solutions, depending on the model used. The most common plate models are the Kirchhoff model and the Mindlin model. The latter is very often referred to as the Reissner-Mindlin one, although the Reissner and the Mindlin models are somewhat different; see e.g. Wang et al. [1].

It is known that the Mindlin solution of the plate problem is very sensitive to the boundary conditions in the neighborhood of the boundary; the solution may vary sharply in the edge-zone. This is called plate boundary layer or plate edge effect, and has been analyzed and discussed by Arnold and Falk [2], [3], Häggblad and Bathe [4] and Babuška and Li [5]. The solution of the Kirchhoff model has no boundary layer. Babuška and Li [5] showed that the boundary layer is present in the solution of the three-dimensional formulation. It therefore corresponds to the physical phenomenon. Arnold and Falk [2], [3] presented a theory for a rigorous analysis of the boundary layer of the Mindlin solution for plates with smooth boundary. The strengths of the boundary layers were found for different boundary conditions for rotations and stress resultants. They illustrated the theory by analyzing the exact solution of a circular and semi-infinite plate with different support conditions. Häggblad and Bathe [4] extended their work to boundary layers near a corner and made comparison of theoretical and numerical results by means of an accurate high-order plate element. Babuška and Li [5] analyzed how well the Mindlin model approximates the three-dimensional formulation. They showed that the quality of the Mindlin solution (with respect to the three-dimensional solution) in the neighborhood of the plate boundary strongly depends on the type of the plate boundary conditions.

The first aim of this work is to discuss the edge effects in the Mindlin solution for rectangular plates with two opposite edges hard-simply supported and the remaining two edges arbitrarily supported (e.g. hard-simple supported, soft-simple supported, hard-clamped, soft-clamped or free). Such plates are usually called Levy plates. We derive analytical (series) Mindlin solution for Levy plates, and further show that it can be represented as the sum of the corresponding Kirchhoff solution, the "shear terms" and the "boundary layer terms". So obtained Mindlin solution is then used to study and illustrate edge effects in rectangular plates for different boundary conditions.

We note that there are several ways to obtain closed or approximate analytical solution for rectangular plates, see e.g. Naumenko et al. [11] for a review on this topic or Nosier et al. [12] for a

series solution. Here we exploit an approach of Lee at al. [13], Reddy and Wang [14] and Lim and Reddy [15], who derived algebraic relationships between the solutions of Mindlin and Kirchhoff plate models. In contrast with the above mentioned works we also consider soft-simply supported and soft-clamped boundary conditions.

Mindlin-theory-based finite elements are very often used for approximate (numerical) analysis of plates. They can effectively approximate the "shear part" of the analytical solution, but they typically have problems to detect the "boundary layer part". Adaptive finite element analysis is needed to make the boundary layer effect visible, see e.g. Selman et al. [6], Lee and Hobbs [7] and Cho and Oden [8]. In conjunction with the mesh refinement algorithm, a (mesh) discretization error indicator/estimator, which is oriented towards capturing the boundary layer effect, has to be used. We note, that the analytical Mindlin solutions, presented in this paper, can be used to estimate performance of any (mesh) discretization error indicator related to the mesh of Mindlin-theory based finite elements; see e.g. Boisse et al. [19], Benoit et al. [20] for examples of discretization error indicators.

The second aim of this work is related to the model error indicator, which is another source of error in the computational (numerical) plate model. It is far more difficult to estimate than the discretization error, see e.g. Stein et al. [10], Bohinc et al. [9]. It is related to the suitability of the mathematical model chosen for the plate analysis. With the analytical solutions for Kirchhoff and Mindlin models available, a suitable model error indicator for the Kirchhoff model can be suggested. We would like to have one that is simple enough as well as sensitive enough to detect the shear layers in plate as well as the edge effects. Having this in mind, we suggest and mutually compare several model error indicators, which have a potential to detect plate regions where Kirchhoff model is fine enough and plate regions where more refined Mindlin model should be used.

The paper is organized as follows. In section 2 we present basic equations of Kirchhoff and Mindlin plate models and algebraic relationship between those two models. We further recall basic results of theoretical edge effect analysis for Mindlin model and discuss several possible model error indicators. In section 3 the results of section 2 are used for the case of Levy plates. In section 4 we present several illustrative examples. The conclusions are drawn in section 5.

2. Plate models

In this section we present basic equations of Kirchhoff and Mindlin plate models and algebraic relationship between them. We recall basic results of edge effect analysis for Mindlin model and introduce several model error indicators.

2.1 The Mindlin and the Kirchhoff plate models and their relationship

Let us consider a plate of thickness h, which mid-plane is in the xy plane. We assume that any transverse loading on the plate can be adequately represented by $q = q(x, y)$. The three basic sets of equations of any structural model (i.e. equilibrium, kinematic and constitutive) are for the Mindlin bending plate model

$$Q_{x,x}^M + Q_{y,y}^M + q = 0, \quad M_{xx,x}^M + M_{xy,y}^M - Q_x^M = 0, \quad M_{yy,y}^M + M_{xy,x}^M - Q_y^M = 0 \tag{1}$$

$$\kappa_{xx}^M = \phi_{x,x}, \quad \kappa_{yy}^M = \phi_{y,y}, \quad 2\kappa_{xy}^M = \phi_{x,y} + \phi_{y,x}$$
$$\gamma_x^M = \phi_x + w_{,x}^M, \quad \gamma_y^M = \phi_y + w_{,y}^M \tag{2}$$

$$M_{xx}^M = D\left(\kappa_{xx}^M + \nu\kappa_{yy}^M\right), \quad M_{yy}^M = D\left(\nu\kappa_{xx}^M + \kappa_{yy}^M\right), \quad M_{xy}^M = \left(\frac{1}{2}D(1-\nu)\right)2\kappa_{xy}^M \tag{3}$$

$$Q_x^M = D^s \gamma_x^M, \quad Q_y^M = D^s \gamma_y^M$$

Here, $M_{xx}^M, M_{yy}^M, M_{xy}^M, Q_x^M, Q_y^M$ are stress resultants, ϕ_x, ϕ_y are rotations of the fibers normal to the mid-plane, w^M is deflection of the mid-plane in the z direction, $\kappa_{xx}^M, \kappa_{xx}^M, 2\kappa_{xy}^M$ are bending strains

(curvatures), γ_x^M, γ_y^M are transverse shear strains, D and D^s are plate constants defined as $D = Eh^3/(12(1-v^2))$, $D^s = \kappa^2 Gh$, G is shear modulus $G = E/(2(1+v))$, E is elastic modulus, v is Poisson's ration, κ^2 is shear correction factor usually set to 5/6 for elastic isotropic plates, and $(\circ)_{,a} = \partial(\circ)/\partial a$. The superscript M relates a quantity with the Mindlin model. Equations (1)-(3) can be reorganized into three coupled differential equations in terms of w^M, ϕ_x, ϕ_y by defining the moment sum $\mathrm{M}^M = (M_{xx}^M + M_{yy}^M)/(1+v) = D(\phi_{x.x} + \phi_{y,y})$, see (3) and (2), and by using the constitutive and the kinematic equations in the equilibrium equations

$$D^s(\nabla^2 w^M + \mathrm{M}^M D^{-1}) = -q$$

$$D^s(\phi_x + w_{,x}^M) = \mathrm{M}^M{}_{,x} + \frac{1}{2}D(1-v)(\phi_{x,y} - \phi_{y,x})_{,y} \tag{4}$$

$$D^s(\phi_y + w_{,y}^M) = \mathrm{M}^M{}_{,y} - \frac{1}{2}D(1-v)(\phi_{x,y} - \phi_{y,x})_{,x}$$

where $\nabla^2 = \partial^2/\partial x^2 + \partial^2/\partial y^2$.

One can replace three coupled equations (4) by a set of two uncoupled differential equations in terms of w^M and $(\phi_{x,y} - \phi_{y,x})$, as shown below. Note that expressions on the right hand side of Eqs. (4)$_2$ and (4)$_3$ can be regarded as "equilibrium shear forces", and those on the left hand side as "constitutive shear forces". By using both types of shear forces in the first equilibrium equation (1)$_1$ one gets the following two equations

$$\nabla^2 \mathrm{M}^M = -q \quad \Rightarrow \quad \nabla^2(\phi_{x,x} + \phi_{y,y}) = -qD^{-1} \tag{5}$$

and

$$D^s(\nabla^2 w^M + \mathrm{M}^M D^{-1}) = -q \tag{6}$$

If M^M in (6) is replaced by (5)$_1$, a 4th order differential equation for the mid-plane displacement w^M is obtained

$$\nabla^4 w^M = (D^{-1} - D^{s-1}\nabla^2)q \tag{7}$$

where $\nabla^4 = \partial^4/\partial x^4 + 2\partial^4/(\partial x^2 \partial y^2) + \partial^4/\partial y^4$. The second equation can be obtained by equating the difference $Q_{x,y}^M - Q_{y,x}^M$ for both types of shear forces to get

$$\nabla^2(\phi_{x,y} - \phi_{y,x}) = c^2(\phi_{x,y} - \phi_{y,x}), \qquad c^2 = \frac{2D^s}{D(1-v)} = \frac{12\kappa^2}{h^2} \tag{8}$$

Equations (7) and (8)$_1$ are two uncoupled differential equations of the Mindlin model for w^M and $(\phi_{x,y} - \phi_{y,x})$. In what follows, we will also use notation

$$\Omega = (\phi_{x,y} - \phi_{y,x}) \tag{9}$$

The coupling between w^M and Ω is achieved through the boundary conditions. If (7) and (8) are solved for some given boundary conditions, the rotations ϕ_x, ϕ_y can be obtained from (4) as

$$\phi_x = -w_{,x}^M + \left(D(-qD^{s-1} - \nabla^2 w^M)_{,x} + \frac{1}{2}D(1-v)(\phi_{x,y} - \phi_{y,x})_{,y}\right)D^{s-1}$$

$$\phi_y = -w_{,y}^M + \left(D(-qD^{s-1} - \nabla^2 w^M)_{,y} - \frac{1}{2}D(1-v)(\phi_{x,y} - \phi_{y,x})_{,x}\right)D^{s-1} \tag{10}$$

The stress resultants can be obtained from (2) and (3).

For the Kirchhoff plate model the equilibrium, kinematic and constitutive equations are

$$Q^K_{x,x} + Q^K_{y,y} + q = 0, \quad M^K_{xx,x} + M^K_{xy,y} - Q^K_x = 0, \quad M^K_{yy,y} + M^K_{xy,x} - Q^K_y = 0 \tag{11}$$

$$\kappa^K_{xx} = -w^K_{,xx}, \quad \kappa^K_{yy} = -w^K_{,yy}, \quad 2\kappa^K_{xy} = -2w^K_{,xy}$$

$$\gamma^K_x = 0, \quad \gamma^K_y = 0 \tag{12}$$

$$M^K_{xx} = D\left(\kappa^K_{xx} + \nu\kappa^K_{yy}\right), \quad M^K_{yy} = D\left(\nu\kappa^K_{xx} + \kappa^K_{yy}\right), \quad M^K_{xy} = \left(\frac{1}{2}D(1-\nu)\right)2\kappa^K_{xy} \tag{13}$$

By inserting constitutive and kinematic equations, (13) and (12), into (11), one can get the following expressions for the "equilibrium shear forces"

$$Q^K_x = -D\left(\nabla^2 w^K\right)_{,x} = M^K_{,x}, \quad Q^K_y = -D\left(\nabla^2 w^K\right)_{,y} = M^K_{,y} \tag{14}$$

where the moment sum is defined as $M^K = \left(M^K_{xx} + M^K_{yy}\right)/(1+\nu) = D\left(w^K_{,xx} + w^K_{,yy}\right) = D\nabla^2 w^K$. The superscript K relates a quantity with the Kirchhoff model. By inserting (14) into (11)$_1$, one can get the familiar 4th order differential equation for the mid-plane displacement of the Kirchhoff model

$$\nabla^2 M^K = -q \quad \Rightarrow \quad \nabla^4 w^K = qD^{-1} \tag{15}$$

Once (15) is solved for some given boundary conditions, the stress resultants can be obtained from (12) and (13). It is clear from (2) and (12) that for the Kirchhoff model $\phi_x = -w^K_{,x}$, $\phi_y = -w^K_{,y}$, and therefore $\Omega = \left(\phi_{x,y} - \phi_{y,x}\right) = 0$.

To solve the boundary value problem of the Mindlin model (i.e. equations (7) and (8)$_1$ for given boundary conditions) one can use an approach of Lee et al. [13], Lim and Reddy [14] and Reddy and Wang [15], who expressed Mindlin solution in terms of the corresponding Kirchhoff solution. In the above mentioned works they exploited the fact that the load q is model independent. Having that in mind, one can set $\nabla^2 M^M = \nabla^2 M^K$, see (5)$_1$ and (15)$_1$, and further

$$M^M = M^K + D\nabla^2\Phi \tag{16}$$

Here $\Phi(x,y)$ is a function, which has to satisfy equation

$$\nabla^4\Phi = 0 \tag{17}$$

By using (16), (15) and $M^K = D\nabla^2 w^K$ in (6), one can obtain the following relationship between the Mindlin and the Kirchhoff mid-plane displacements as

$$w^M = w^K + \underline{M^K D^{s^{-1}} + \psi - \Phi} \tag{18}$$

Here $\psi(x,y)$ is a function, which has to satisfy equation

$$\nabla^2\psi = 0 \tag{19}$$

It is clear from (18) that solution of the first differential equation of the Mindlin model (7) can be replaced by solutions of the three differential equations (15)$_2$, (17) and (19), which might be easier to solve. In view of (9) we also write the second uncoupled differential equation of the Mindlin model (8)$_1$ as

$$\underbrace{\frac{h^2}{12\kappa^2}}_{c^{-2}}\nabla^2\Omega - \Omega = 0 \tag{20}$$

If equations (15)$_2$, (17), (19) and (20) are solved for some given boundary conditions (note, that Φ, ψ and Ω depend both on displacement/rotation boundary conditions and loading), one can get with (4), (16) and (18) the following expressions for rotations

$$\phi_x = -w^K,_x + \left(DD^{s-1}\left(\nabla^2\Phi\right) + \Phi - \psi\right),_x + \underline{\underline{c^{-2}\Omega,_y}}$$

$$\phi_y = -w^K,_y + \left(DD^{s-1}\left(\nabla^2\Phi\right) + \Phi - \psi\right),_y - \underline{\underline{c^{-2}\Omega,_x}} \tag{21}$$

By inserting (18) and (21) into (2) and (3), one can finally obtain expressions for the Mindlin stress resultants in such a way that they already include Kirchhoff stress resultants (12) and (13)

$$M_{xx}^M = M_{xx}^K - D(1-\nu)\Lambda_{1,y} + \underline{D\nabla^2\Phi}, \quad M_{yy}^M = M_{yy}^K - D(1-\nu)\Lambda_{2,x} + \underline{D\nabla^2\Phi}$$

$$M_{xy}^M = M_{xy}^K + \frac{1}{2}D(1-\nu)\left(\Lambda_{1,x} + \Lambda_{2,y}\right) \tag{22}$$

$$Q_x^M = Q_x^K + \underline{D\left(\nabla^2\Phi\right),_x} + \underline{\underline{\frac{D(1-\nu)}{2}\Omega,_y}}, \quad Q_y^M = Q_y^K + \underline{D\left(\nabla^2\Phi\right),_y} - \underline{\underline{\frac{D(1-\nu)}{2}\Omega,_x}}$$

where

$$\Lambda_1 = \left(DD^{s-1}\nabla^2\Phi + \Phi - \psi\right),_y - \underline{\underline{c^{-2}\Omega,_x}}, \quad \Lambda_2 = \left(DD^{s-1}\nabla^2\Phi + \Phi - \psi\right),_x + \underline{\underline{c^{-2}\Omega,_y}}$$

$$\Lambda_{1,x} + \Lambda_{2,y} = 2\left(DD^{s-1}\nabla^2\Phi + \Phi - \psi\right),_{xy} + \underline{\underline{\Omega - 2c^{-2}\Omega,_{xx}}} \tag{23}$$

As shown e.g. by Arnold and Falk [2], [3] or Häggblad and Bathe [4], Mindlin rotations and stress resultants can have a sharp change in behavior near the plate edge (i.e. edge effect or boundary layer effect). It is known that the biharmonic differential equation does not have such an edge effect. Since the Kirchhoff part and the "shear part" are related to biharmonic equations, see (15) and (7), they are not responsible for the edge effect. It follows from (18) that ψ and Φ are not responsible for the edge effect either. It is therefore Ω alone, which governs the edge-zone behavior of rotations and stress resultants. We can conclude from the above that the Mindlin solution can be seen as a sum of three parts: *(i)* the Kirchhoff solution, *(ii)* the "shear part" of the solution, which includes ψ and Φ functions (the single underlined terms in the above equations), and *(iii)* the Ω function part or the "boundary layer part" of the solution (the double underlined terms in the above equations).

2.2 Boundary layer in the solution of the Mindlin model

As discussed above, it is the Ω function that is responsible for the boundary layer. It can be interpreted as the local transverse twist, see (9). By examining eq. (20), we can conclude that the term $\nabla^2\Omega$ has an increasingly smaller role for decreasing h. Therefore, for thin plates Ω is considerably different from zero only near the boundary. For decreasing h the "shear part" of the solution also tends towards zero. Thus, for thin plates the part *(ii)* of the solution is very small and the part *(iii)* of the solution is negligible in the interior of the plate. In such a case the Mindlin solution can be seen as the perturbed Kirchhoff solution. For that reason Häggblad and Bathe [4], see also Arnold and Falk [2], [3], assumed the following asymptotic expansions of w^M and Ω in powers of h

$$w^M = w^K + hw_1 + h^2w_2 + \dots$$

$$\Omega = \Omega_{00} + \chi\left(\Omega_0 + h\Omega_1 + h^2\Omega_2 + \dots\right) \tag{24}$$

where χ is a cut-off function equal to one in the edge-zone and zero outside that region, $\Omega_i = \overline{\Omega}_i(\rho/h, s)e^{-c\rho}$ are boundary layer functions, ρ, s are boundary fitted coordinates (ρ is distance from the point under consideration to the nearest point on the boundary curve and s is arc-length parameter of that point). For Kirchhoff solution $\Omega = 0$.

With the above expansions Arnold and Falk [2], [3] and Häggblad and Bathe [4] subsequently solved Mindlin plate boundary value problems and evaluated relative strengths of Ω function, rotations and stress resultants for smooth edge curves and for different boundary conditions. Their results are summarized in Table 1. The strength is related to the power of the first non-vanishing term

in the solution. Note, that stress resultants in Table 1 are defined as $\overline{M}_{nn} = M_{nn}^M / D$, $\overline{Q}_s = Q_s^M / D$, etc., where coordinate n has an opposite direction of ρ. No boundary layer exists for transverse displacement. Neither there is a boundary layer for hard-simply supported and soft-clamped straight (i.e. zero curvature) edges.

2.3 Model error indicator

When analyzing plates it is interesting to have an information weather the chosen model is an adequate one, i.e., weather it does or does not produce non-desirable high error (at some regions of the plate) with respect to the solution of the model that we a priori know that it performs better (in comparison with the 3d solid model) then the chosen one. To evaluate the model error, one thus has to have solutions of two hierarchical models, where the hierarchy is defined with respect to the 3d model.

Concerning the present problem, we a priori know that the Mindlin solution is closer to the 3d solution than the Kirchhoff one. If one has both Kirchhoff and Mindlin solutions available for the same plate problem (as this is the case here, since the latter solution incorporates the former one), a model error indicator for the Kirchhoff model can be defined as the difference between those two solutions. The difference can be written in a form of normalized energy norm, i.e. as

$$\eta^{MK} = \frac{\Delta \mathbf{F}^{MK} \mathbf{D}^{-1} \Delta \mathbf{F}^{MK}}{\mathbf{F}^M \mathbf{D}^{-1} \mathbf{F}^M} \tag{25}$$

The indicator η^{MK} in (25) shows how apart are the solutions (in an energy sense) at a certain point of the plate. One can choose vector $\Delta \mathbf{F}^{MK}$ to represent the difference between the Mindlin and the Kirchhoff "constitutive stress resultants" and vector $\mathbf{F}^M$ to represent the stress resultants of the Mindlin model

$$\Delta \mathbf{F}^{MK} = \Delta \mathbf{F}^{MK,cons} = \left[M_{xx}^M - M_{xx}^K, M_{yy}^M - M_{yy}^K, M_{xy}^M - M_{xy}^K, Q_x^M, Q_y^M \right]^T$$
$$\mathbf{F}^M = \left[M_{xx}^M, M_{yy}^M, M_{xy}^M, Q_x^M, Q_y^M \right]^T \tag{26}$$

Matrix $\mathbf{D}$ is the plate constitutive matrix

$$\mathbf{D} = \begin{bmatrix} D & \nu D & 0 & 0 & 0 \\ \nu D & D & 0 & 0 & 0 \\ 0 & 0 & D(1-\nu)/2 & 0 & 0 \\ 0 & 0 & 0 & D^s & 0 \\ 0 & 0 & 0 & 0 & D^s \end{bmatrix} \tag{27}$$

In such a case it is the shear part of the plate bending energy that characterizes the difference between the Kirchhoff and the Mindlin model in (25), since the "constitutive shear forces" of the Kirchhoff model are zero. We denote model error indicator based on (26) and (25) as $\eta^{MK,cons}$

$$\eta^{MK,cons} = \frac{\Delta \mathbf{F}^{MK,cons} \mathbf{D}^{-1} \Delta \mathbf{F}^{MK,cons}}{\mathbf{F}^M \mathbf{D}^{-1} \mathbf{F}^M} \tag{28}$$

Alternatively, the "equilibrium shear stress resultants" of the Kirchhoff model Q_x^K and Q_y^K can be included in vector $\Delta \mathbf{F}^{MK}$ in (25), i.e.

$$\Delta \mathbf{F}^{MK} = \Delta \mathbf{F}^{MK,equil} = \left[M_{xx}^M - M_{xx}^K, M_{yy}^M - M_{yy}^K, M_{xy}^M - M_{xy}^K, Q_x^M - Q_x^K, Q_y^M - Q_y^K \right]^T \tag{29}$$

We denote such error indicator as $\eta^{MK,equil}$

$$\eta^{MK,equil} = \frac{\Delta \mathbf{F}^{MK,equil} \mathbf{D}^{-1} \Delta \mathbf{F}^{MK,equil}}{\mathbf{F}^M \mathbf{D}^{-1} \mathbf{F}^M} \tag{30}$$

It takes into account only the "shear part" and the "boundary layer part" of the Mindlin solution, see (22) and (23). However, it is usually not sensitive enough, since the difference between the "equilibrium" Mindlin and Kirchhoff stress resultants is rather small in general.

One can also consider the difference between the Mindlin and the Kirchhoff "constitutive moments" as small in comparison to the difference between the Mindlin and the Kirchhoff "constitutive shear forces". The model indicator η^{MK} in (25) can be therefore replaced by the following one

$$\eta^M = \frac{\mathbf{Q}^M \mathbf{D}^{s-1} \mathbf{Q}^M}{\mathbf{F}^M \mathbf{D}^{-1} \mathbf{F}^M} \tag{31}$$

where $\mathbf{Q}^M$ and $\mathbf{D}^s$ are given as

$$\mathbf{Q}^M = \left[Q_x^M, Q_y^M \right]^T, \qquad \mathbf{D}^s = \begin{bmatrix} D^s & 0 \\ 0 & D^s \end{bmatrix} \tag{32}$$

The indicator (31) is approximation of (28). It is again characterized by the shear part of the plate bending energy, but it only party takes into account (through the shear forces) the "shear part" of the Mindlin solution as well as its "boundary layer part".

One can also try to indicate the error of the Kirchhoff model by solution of this model only, i.e. by

$$\eta^K = \frac{\mathbf{Q}^K \mathbf{D}^{s-1} \mathbf{Q}^K}{\mathbf{F}^K \mathbf{D}^{-1} \mathbf{F}^K} \tag{33}$$

where $\mathbf{Q}^K = \left[Q_x^K, Q_y^K \right]^T$ and $\mathbf{F}^K = \left[M_{xx}^K, M_{yy}^K, M_{xy}^K, Q_x^K, Q_y^K \right]^T$. As shown below in numerical examples, such error indicator is not very reliable, since Kirchhoff stress resultants do not carry any information about the boundary layer effects and the "shear effects", which are intrinsic only to the Mindlin solution.

3. Rectangular Levy plates

In this section we use the above results for the case of Levy plates.

3.1 Mindlin solution

Let us consider a rectangular plate of constant thickness h, which mid-surface occupies region $\{(x, y) \mid x \in [0, a], y \in [-b/2, b/2]\}$. It has two opposite edges at $x = 0$ and $x = a$ hard-simply supported, and the remaining two edges arbitrarily supported (hard- or soft-simply supported, hard- or soft-clamped or free). It is assumed that any loading q can be described by a single Fourier series as

$$q(x, y) = \sum_{m=1}^{\infty} q_m(y) \sin \alpha_m x \tag{34}$$

where $\alpha_m = m\pi a^{-1}$. In what follows we will restrict ourselves to a case where $q(x, y)$ is constant or linear function with respect to y.

In order to obtain the Kirchhoff solution, the following series for displacements is assumed

$$w^K(x, y) = \sum_{m=1}^{\infty} W_m^K(y) \sin \alpha_m x \tag{35}$$

that satisfies simply supported boundary conditions at $x = 0$ and $x = a$, i.e. $w^K = M_{xx}^K = 0$. Note, that the Kirchhoff model defines simple supports as hard-simple supports, see e.g. Babuška and Lee [5]. By using (22) and (23) in (15)$_2$, an ordinary 4th order differential equation with constant coefficients is obtained for each m

$$W_m^K(y) = (A_{1m} + A_{2m}y)\cosh\alpha_m y + (A_{3m} + A_{4m}y)\sinh\alpha_m y + q_m(D\alpha_m^4)^{-1} \tag{36}$$

Here A_{im} (i=1,4) are constants that are determined from the boundary conditions at $y = \pm b/2$. Two boundary conditions are defined at each edge, see Table 2. In this work the constants A_{im} have been obtained by using symbolic mathematical computer code *Mathematica* [16], but they can be also found in textbooks on Kirchhoff plates, see e.g. Reddy [17]. Once A_{im} are known, the displacement and stress resultants of the Kirchhoff model follow from (36), (35), (12) and (13).

In order to get Mindlin solution as an extension of the Kirchhoff solution, one can choose displacement and rotations of the form

$$w^M(x,y) = \sum_{m=1}^{\infty} W_m^M(y)\sin\alpha_m x$$

$$\phi_x(x,y) = \sum_{m=1}^{\infty}\varphi_{xm}(y)\cos\alpha_m x, \quad \phi_y(x,y) = \sum_{m=1}^{\infty}\varphi_{ym}(y)\sin\alpha_m x \tag{37}$$

Expressions (37) are in accordance with the hard-simply supported boundary conditions at $x = 0$ and $x = a$, i.e. $w^M = M_{xx}^M = \phi_y = 0$. In the next step one has to define appropriate expressions for Φ, ψ and Ω. We recall that those functions have to: *(i)* satisfy differential equations (17), (19) and (20), and *(ii)* enable hard-simple support boundary conditions at $x = 0$ and $x = a$ when inserted in (21) and (18). Note, that *(ii)* is identical to the requirement that rotations ϕ_x, ϕ_y and displacement w^M are written in the form (37), when expressions for Φ, ψ and Ω are introduced in (21) and (18). It can be proven that the following functions are consistent with the above demands

$$\Phi(x,y) = \sum_{m=1}^{\infty}\frac{y}{2\alpha_m}(C_{1m}\cosh\alpha_m y + C_{2m}\sinh\alpha_m y)\sin\alpha_m x = \sum_{m=1}^{\infty}\Phi_m$$

$$\psi(x,y) = \sum_{m=1}^{\infty}(C_{3m}\cosh\alpha_m y + C_{4m}\sinh\alpha_m y)\sin\alpha_m x = \sum_{m=1}^{\infty}\psi_m \tag{38}$$

$$\Omega(x,y) = \sum_{m=1}^{\infty}(C_{5m}\sinh\lambda_m y + C_{6m}\cosh\lambda_m y)\cos\alpha_m x = \sum_{m=1}^{\infty}\Omega_m$$

Here $\lambda_m^2 = \alpha_m^2 + c^2$, where constant c^2 is defined in (8)$_2$. C_{im} (i=1,6) are unknown constants that are to be determined from the Mindlin model boundary conditions at $y = \pm b/2$. Three boundary conditions are needed at each edge; see Table 2 for their explicit expressions.

In the present work the constants C_{im} have been obtained for boundary conditions from Table 2 by using *Mathematica* [16]. The expressions are lengthy and can be for Levy plates with symmetrical loading for hard-simple supported, hard-clamped and free edges found elsewhere, see e.g. Lee et al. [13] or Reddy and Wang [14]. To be complementary with the above mentioned works, we provide in Appendix only the constants C_{im} for soft-simple supported and soft-clamped edges. The constants in Appendix are valid for any symmetric loading with respect to $y = 0$ that can be expressed in form (34). Note, that for such loading $C_{1m} = C_{4m} = C_{6m} = 0$, independently of the type of boundary conditions.

Once C_{im} are obtained, the functions (38) become complete. They can be used, together with the corresponding Kirchhoff solution, in (21), (18) and (22) to evaluate Mindlin rotations, displacement and stress resultants, respectively. The coefficients $\varphi_{xm}(y)$, $\varphi_{ym}(y)$ and $W_m^M(y)$ can be also easily evaluated. We note, that for SH-SS plate and for SH-CS plate the corresponding Kirchhoff solutions are of hard type, since there are no soft-simple supported and no soft-clamped Kirchhoff results.

3.2 Boundary layer

Arnold and Falk [2] showed that for hard-simply supported and soft-clamped boundary conditions there are no edge effects for edges with zero curvature (i.e. for straight edges). Accordingly, in rectangular plates under consideration no edge effects are expected at $x = 0$ and $x = a$, while edge effects should be observed at $y = \pm b/2$ for soft-simply supported, hard-clamped and free boundary conditions. No edge effects should be observed at $y = \pm b/2$ for hard-simply supported and soft-clamped boundary conditions.

With respect to Table 1 we have at $y = \pm b/2$ $n = y$ and $s = x$. We therefore expect very strong edge effect for Q_x in SH-SS and SH-F plates, strong edge effects for Q_y and M_{xy} in SH-SS and SH-F plates and weaker edge effects for other quantities of SH-SS, SH-F and SH-CH plates. In general we expect strong edge effects in SH-SS and SH-F plates and weak edge effects in SH-CH plate.

3.3 Model error indicator and thickness sensitivity

With analytical solutions available for both the Kirchhoff and the Mindlin model, one can easily compute the model error indicators (28), (30), (31) and (33) at each point of the plate.

Moreover, one can also compute sensitivity of the Mindlin stress resultant on the thickness. Note, that the Kirchhoff solution does not depend on the thickness h (except through the factor h^3), while the Mindlin solution depends on the thickness in a complicated way. One may thus define

$$M_{xxh}^M = \frac{\partial M_{xx}^M(x,y,h)}{\partial h}, \quad Q_{xh}^M = \frac{\partial Q_x^M(x,y,h)}{\partial h}, \quad \ldots \tag{39}$$

to check sensitivity of stress resultants on the thickness.

4. Examples
4.1 Exact solution for a sinusoidal loading

As a first illustrative example we consider a square plate $a = b = 1$, $E = 10^6$, $\kappa^2 = 5/6$, $\nu = 0.3$, $h = 10^{-2}$, loaded by $q = q_0 \sin \pi x a^{-1}$, $q_0 = 1$. Boundary conditions at the edges $x = 0$, $x = a$ are of hard-simply supported type, and boundary conditions at the remaining two edges at $y = \pm b/2$ are listed in Table 2. For the chosen loading the exact analytical Mindlin and Kirchhoff solutions can be obtained by using a single term, i.e. $m = 1$.

With this example we illustrate edge effects in rectangular plates. According to Table 1 one should expect strong boundary layer at F and SS edges, and weak boundary layer at CH edge. Since the boundary layer appears only in Mindlin solution, it can be presented as the difference between the Mindlin and the Kirchhoff solution. Such presentation is shown for SH-F plate in Figure 2. It can be clearly seen from Figure 2 that sharp solution differences appear in the vicinity of the edges (although the values may be small in an absolute manner). Away from the boundary layer the two solutions are very similar; they differ only for the "shear part" (see the single underlined terms in (21)-(23)). Edge effect is observed for all quantities except for w^M and ϕ_y, which is in accordance with Table 1.

Figures 3 and 4 further show the Mindlin internal forces in a plate section $x = const.$ near the boundary $y = b/2$ for three different ratios h/a (the coordinate ρ is defined as $\rho = b/2 - y$). The results are for SH-F, HS-CH and HS-SS plates, respectively, and are in agreement with Table 1. The strongest boundary layer at the F edge (Figure 3) exhibits the shear force in the direction tangential to the edge Q_x^M, weaker edge effect is observed for Q_y^M and M_{xy}^M, and the weakest for M_{xx}^M and M_{yy}^M. The same order of the boundary layer stress resultants strengths is observed also for CH and SS edges (Figure 4), although edge effects at CH edge are not as strong as at F and SS edges.

Stress resultants of Mindlin solution are complicated functions of thickness h, which can be illustrated by plotting their derivatives with respect to h (we call them sensitivities). Figure 5 shows sensitivities of some stress resultants for SS edge. It is interesting to see that sharp variations of sensitivities are observed in the edge zone, and that sensitivities have equal and almost constant value outside that zone for all h/a ratios.

4.2 Approximate solution for uniform loading

In this section we present Mindlin results for a square plate $a = b$ with $h/a = 0.2$, $\nu = 0.3$, $\kappa^2 = 5/6$ and uniform loading $q = q_0$. We compare our results with those of Lee at el. [13] and Kant and Hinton [18] in Tables 3, 4 and 5, and we show some new results in Table 6. It can be seen that the present results are in very good agreement with the compared ones when the chosen number of harmonics is 40.

4.3 Estimation of model error for a square plate under uniform loading

With this example we estimate model error for a square plate $a = b$ with $h/a = 0.1$, $\nu = 0.3$, $\kappa^2 = 5/6$ and uniform loading $q = q_0$. The number of harmonics is 40.

The results are presented in Figures 6-8. Figure 6 shows contour plots of model error indicators (28), (31) and (33), and Fig. 7 shows 3d plots of the same indicators. It can be seen from those two figures that indicator (28) and its approximation (31) yield very similar results, except for the SH-CH plate, where the corner values of indicator (28) are badly approximated by indicator (31). The reason for this is neglection of the "shear part" and the "boundary layer part" of the Mindlin moments in (31). Recall that those effects were only included through the Mindlin shear forces, although it seems that in this case they have considerable influence on the Mindlin moments as well. It can be also seen from Figs 6 and 7 that indicator (33) fails to represent the shape of indicator (28) in the case of SH-SS and SH-F plates. This is expected, since those two plates have the strongest boundary layer effect, which cannot be captured by Kirchhoff solution used in (33). On the other hand, (28) and (33) are similar for the case of SH-SH and SH-CS plates, which do not have the boundary layer. The Kirchhoff shear energy indicator (33) is also not capable to distinguish between the soft and the hard supports. We can conclude from this example that the model error indicator (31) is reasonable approximation of (28), and that the model error indicator (33) is not reliable.

In Figure 8 we present energy norm of the "shear part" and the "boundary layer part" of the Mindlin solution, which is expressed by the indicator (30). It can be seen that the value of (30) is zero over the entire domain for SH-SH plate, and is non-zero only at the corners of SH-CS plate (which has no boundary layer) and SH-CH plate (which has weak boundary layer). This model error indicator shows the difference (expressed in an energy norm) between the "equilibrium stress resultants" of the Mindlin and the Kirchhoff models.

5. Conclusions

The Fourier series solutions were derived for Mindlin and Kirchhoff plate models in the case of rectangular Levy plates. For a specified boundary value problem the equations of both models were solved simultaneously and the results of the Mindlin model were expressed by using the Kirchhoff results. The terms in the expressions for the Mindlin rotations and stress resultants were identified that are related to the edge effects and to the shear constraint relaxation. The model error indicators were suggested to find regions of the plate where Kirchhoff model is adequate and more refined Mindlin model should be used.

The chosen examples illustrate behavior of stress resultants in the boundary layer for different thickness to span ratios and for different boundary conditions as well as sensitivity of the stress resultants on plate thickness. It has been also shown by the examples that the derived analytical solutions can be useful for testing the discretization error as well as the modeling error indicators derived within the adaptive finite element analysis of plates.

Appendix

Mindlin constants for soft-simply supported plate at $y = \pm b/2$ and for symmetric loading with respect to $y = 0$ are:

$$C_{1m} = C_{4m} = C_{6m} = 0$$

$$C_{2m} = \frac{D^s q_m \lambda_m (-1 + v) Cosh\left(\dfrac{b\lambda_m}{2}\right) Sech\left(\dfrac{b\alpha_m}{2}\right)(-b\alpha_m + Sinh(b\alpha_m))}{D\alpha_m F_{1m}}$$

$$C_{3m} = \frac{D^s b q_m \lambda_m (-1 + v) Cosh\left(\dfrac{b\lambda_m}{2}\right) Sech\left(\dfrac{b\alpha_m}{2}\right)(b\alpha_m - Sinh(b\alpha_m)) Tanh\left(\dfrac{b\alpha_m}{2}\right)}{4D\alpha_m^2 F_{2m}}$$

$$C_{5m} = \frac{c^2 q_m \gamma_m (b\alpha_m - Sinh(b\alpha_m))}{D\alpha_m^2 F_{1m}}$$

where

$$F_{1m} = -F_{2m} = -\delta_m Cosh\left(\frac{b\lambda_m}{2}\right) Sinh\left(\frac{b\alpha_m}{2}\right)\left(\eta_m Cosh\left(\frac{b\alpha_m}{2}\right) - \xi_m Sinh\left(\frac{b\alpha_m}{2}\right)\right) +$$

$$Cosh\left(\frac{b\alpha_m}{2}\right)^2\left(-\zeta_m Cosh\left(\frac{b\lambda_m}{2}\right) + \gamma_m \varepsilon_m Sinh\left(\frac{b\lambda_m}{2}\right)\right)$$

and

$$\gamma_m = -D^s + D\alpha_m^2(-1 + v), \quad \delta_m = \alpha_m \lambda_m(-1 + v), \quad \varepsilon_m = 2(c^2 + 2\alpha_m^2), \quad \xi_m = D^s b\alpha_m,$$

$$\eta_m = 2(2D\alpha_m^2 + D^s), \quad \zeta_m = D^s b\alpha_m^2 \lambda_m(-1 + v)$$

Mindlin constants for soft-clamped plate at $y = \pm b/2$ and for symmetric loading with respect to $y = 0$ are:

$$C_{1m} = C_{4m} = C_{5m} = C_{6m} = 0$$

$$C_{2m} = \frac{4q_m Sinh\left(\dfrac{b\alpha_m}{2}\right)(-b\alpha_m + Sinh(b\alpha_m))}{F_{3m}}$$

$$C_{3m} = \frac{q_m\left(\xi_m Cosh\left(\dfrac{b\alpha_m}{2}\right) + \eta_m Sinh\left(\dfrac{b\alpha_m}{2}\right)\right)(-b\alpha_m + Sinh(b\alpha_m))}{D^s \alpha_m^2 F_{3m}}$$

where

$$F_{3m} = (b\alpha_m + Sinh(b\alpha_m))\left(\xi_m + \frac{\eta_m}{2} Sinh(b\alpha_m)\right)$$

References

[1] Wang CM, Lim GT, Reddy JN, Lee KH. Relationships between bending solutions of Reissner and Mindlin plate theories. Engineering Structures 2001; 23:838-849.
[2] Arnold DN, Falk RS. Edge effects in the Reissner-Mindlin plate theory. In: Noor AK, Belytschko T, Simo JC, editors. Analytical and computational models for shells, ASME, 1989. p. 71-90.

[3]   Arnold DN, Falk RS. The boundary layer for the Reissner-Mindlin plate model. SIAM J. Math. Anal. 1990; 21:281-312.

[4]   Häggblad B, Bathe KJ. Specifications of boundary conditions for Reissner/Mindlin plate bending finite elements. Int. J. Numer. Methods Engng. 1990; 30:981-1012.

[5]   Babuška I, Li L. The problem of plate modeling: Theoretical and computational results. Comput. Methods Appl. Mech. Eng. 1992; 100:249-273.

[6]   Selman A, Hinton E, Atamaz-Sibai W. Edge effects in Mindlin-Reissner plates using adaptive mesh refinement. Eng. Comput. 1990; 7:217-226.

[7]   Lee CK, Hobbs RE. Automatic adaptive refinement for plate bending problems using Reissner-Mindlin plate bending elements. Int. J. Numer. Methods Engng. 1998; 41:1-63.

[8]   Cho J-R, Oden JT. Locking and boundary layer in hierarchical models for thin elastic structures. Comput. Methods Appl. Mech. Eng. 1997; 149:33-48.

[9]   Bohinc U, Ibrahimbegović A, Brank B. Model adaptivity for finite element analysis of thick and thin plates based on equilibrated boundary stress resultants. Computers and Structures 2007; submitted.

[10] Stein E, Rüter M, Ohnimus S. Adaptive finite element analysis and modeling of solids and structures. Findings, problems and trends. Int. J. Numer. Methods Engng. 2004; 60:103-138.

[11] Naumenko K, Altenbach J, Altenbach H, Naumenko VK. Closed and approximate analytical solutions for rectangular Mindlin plates. Acta Mechanica 2001; 147: 153-172.

[12] Nosier A, Yavari A, Sarkani S. A study of the edge-zone equation of Reissner-Mindlin plate theory in bending of laminated rectangular plates. Acta Mechanica 2001; 146: 227-238.

[13] Lee KH, Lim GT, Wang CM. Thick Levy plates re-visited. Int. J. of Solids and Structures 2002; 39:127-144.

[14] Reddy JN, Wang CM. An overview of the relationships between solutions of classical and shear deformation plate theories. Composite Science and Technology 2000; 60:2327-2335.

[15] Lim GT, Reddy JN. On canonical bending relationships for plates. Int. J. of Solids and Structures 2003; 40:3039-3067.

[16] Mathematica.Wolfram Research Inc.

[17] Reddy JN. Theory and analysis of elastic plates. Taylor & Francis, 1999.

[18] T. Kant, E. Hinton, Numerical analysis of rectangular Mindlin plates by segmentation method. Civil Engineering Department Report C/R/365/80, University of Wales, Swansea.

[19] P. Boisse, S. Perrin, G. Coffignal, K. Hadjeb, Error estimation through the constitutive relation for Reissner-Mindlin plate bending finite elements. Computers and Structures 1999; 73:615-627.

[20] C. Benoit, P. Coorevits, J.-P. Pelle, Error estimation for plate structures. Application using the DKT element. Eng. Comput. 1999; 16:584-600.

Table 1. Strengths of Ω function, rotations and stress resultants

	Ω	ϕ_s	ϕ_n	$\overline{M}_{nn}$	$\overline{M}_{ss}$	$\overline{M}_{sn}$	$\overline{Q}_s$	$\overline{Q}_n$
Soft-simply supported	0	1	2	1	1	0	-1	0
Hard-simply supported	1	2	3	2	2	1	0	1
Soft-clamped	2	3	4	3	3	2	1	2
Hard-clamped	1	3	4	3	3	2	1	2
Free	0	1	2	1	1	0	-1	0

Table 2. Boundary conditions for Levy plates at $y = \pm b / 2$.

Boundary conditions	Plate description	Kirchhoff model	Mindlin model
Soft-simply supported	SH-SS		$w^M = M_{yy}^M = M_{xy}^M = 0$
Hard-simply supported	SH-SH	$w^K = M_{yy}^K = 0$	$w^M = M_{yy}^M = \phi_x = 0$
Soft-clamped	SH-CS		$w^M = \phi_y = M_{xy}^M = 0$
Hard-clamped	SH-CH	$w^K = w_{,y}^K = 0$	$w^M = \phi_x = \phi_y = 0$
Free	SH-F	$M_{yy}^K = Q_y^K + M_{xy,x}^K = 0$	$M_{yy}^M = Q_y^M = M_{xy}^M = 0$

Table 3. Non-dimensional results for SH-SH plate; absolute values.

$(x/a;y/a)$	Stress resultant	Present (m=40)	Present (m=20)	Lee et al. [13] (m=40)	Kant & Hinton [18]
(0.5;0)	$M_{xx}^M /(q_0 a^2)$	0.047885	0.047878	0.0479	0.0479
(0.5;0)	$M_{yy}^M /(q_0 a^2)$	0.047886	0.047884	0.0479	0.0478
(1;0.5)	$M_{xy}^M /(q_0 a^2)$	0.032475	0.033246	0.0325	0.0324
(1;0)	$Q_x^M /(q_0 a)$	0.332592	0.327534	0.333	0.332
(0.5;0.5)	$Q_y^M /(q_0 a)$	0.337531	0.337154	0.338	0.337
(0.5;0)	$w^M D /(q_0 a^4)$	0.004904	0.004904	0.004904	0.0049

Table 4. Non-dimensional results for SH-CH plate; absolute values.

$(x/a;y/a)$	Stress resultant	Present (m=40)	Present (m=20)	Lee et al. [13] (m=40)	Kant & Hinton [18]
(0.5;0)	$M_{xx}^M /(q_0 a^2)$	0.029210	0.029204	0.0292	0.0292
(0.5;0)	$M_{yy}^M /(q_0 a^2)$	0.033053	0.033051	0.0331	0.0330
(0.5;0.5)	$M_{yy}^M /(q_0 a^2)$	0.062687	0.062685	0.0627	0.0626
(1;0)	$Q_x^M /(q_0 a)$	0.251206	0.246148	0.251	0.251
(0.5;0.5)	$Q_y^M /(q_0 a)$	0.474938	0.474558	0.475	0.475
(0.5;0)	$w^M D /(q_0 a^4)$	0.003021	0.003021	0.003021	0.002930

Table 5. Non-dimensional results for SH-F plate; absolute values.

(x/a;y/a)	Stress resultant	Present (m=40)	Present (m=20)	Lee et al. [13] (m=40)	Kant & Hinton [18]
(0.5;0)	$M_{xx}^{M}/(q_0a^2)$	0.122924	0.122917	0.123	0.123
(0.5;0)	$M_{yy}^{M}/(q_0a^2)$	0.023722	0.023720	0.0237	0.0237
(1;0)	$Q_{x}^{M}/(q_0a)$	0.456581	0.451523	0.457	0.456
(0.5;0)	$w^{M}D/(q_0a^4)$	0.014539	0.014539	0.014539	0.014496

Table 6. Non-dimensional results for SH-SS and SH-CS plate; absolute values.

(x/a;y/a)	Stress resultant	Present (m=40)	Present (m=40)
		SH-SS	SH-CS
(0.5;0)	$M_{xx}^{M}/(q_0a^2)$	0.051500	0.029795
(0.5;0)	$M_{yy}^{M}/(q_0a^2)$	0.050762	0.033525
(1;0.25)	$M_{xy}^{M}/(q_0a^2)$	0.020854	0.012484
(1;0)	$Q_{x}^{M}/(q_0a)$	0.348294	0.253811
(0.5;0.5)	$Q_{y}^{M}/(q_0a)$	0.403499	0.505320
(0.5;0)	$w^{M}D/(q_0a^4)$	0.00527	0.003081
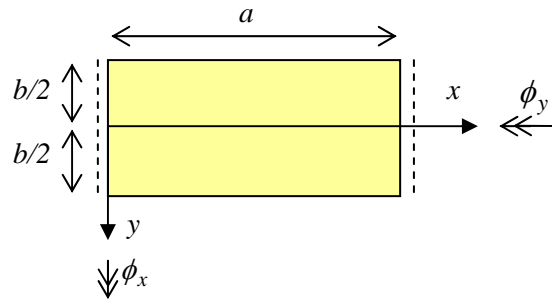
Figure 1. Levy plate: notation.
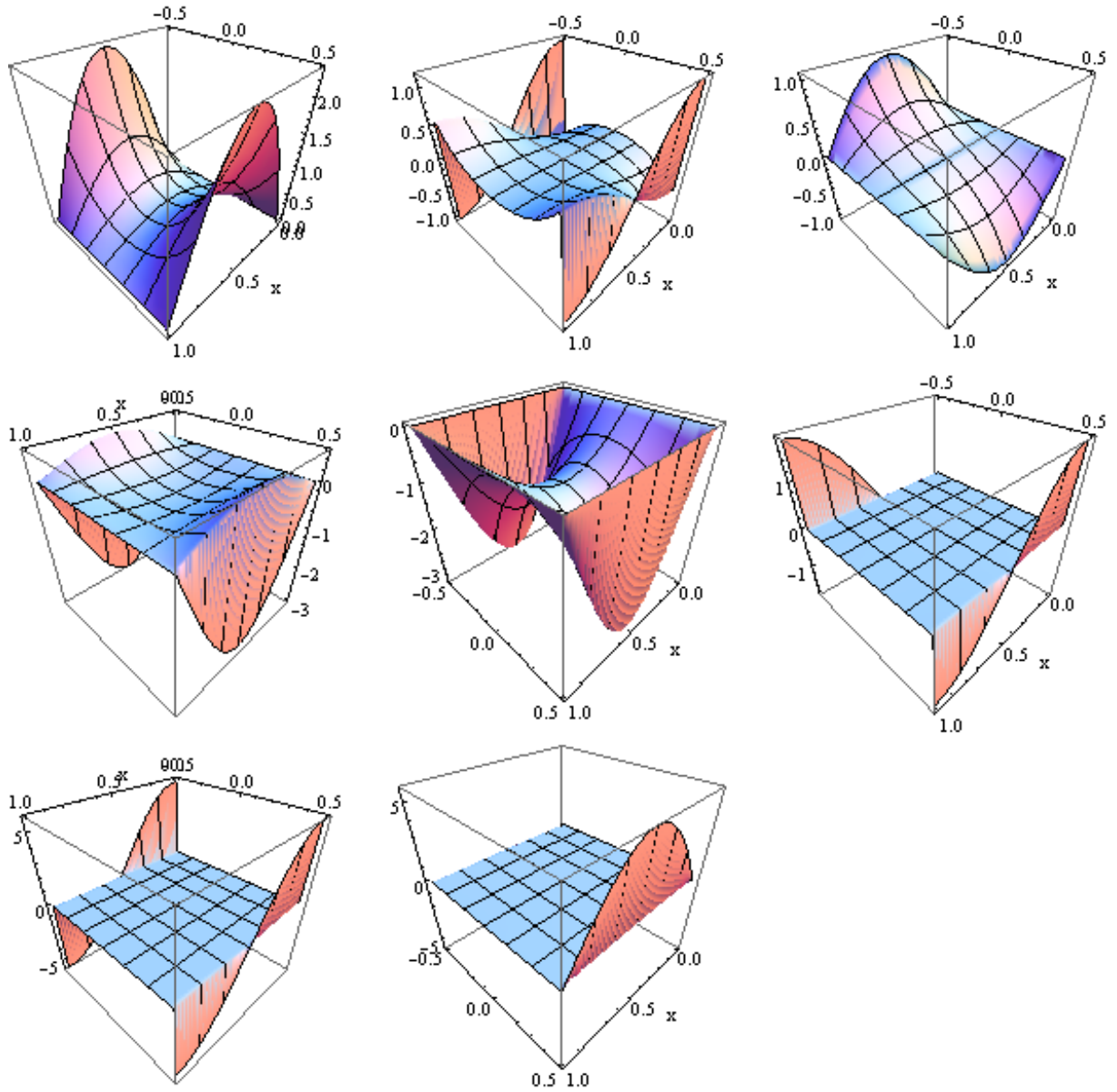
Figure 2. Square SH-F plate. Difference between the Mindlin and the Kirchhoff solutions. Top, from left to right: (a) $(w^M - w^K)10^{-4}$, (b) $(\phi_x - (-w_{,x}^K))10^{-3}$, (c) $(\phi_y - (-w_{,y}^K))10^{-3}$. Middle, from left to right: (d) $(M_{xx}^M - M_{xx}^K)10^{-4}$, (e) $(M_{yy}^M - M_{yy}^K)10^{-4}$, (f) $(M_{xy}^M - M_{xy}^K)10^{-2}$. Bottom, from left to right: (g) $Q_x^M - Q_x^K$, (h) $(Q_y^M - Q_y^K)10^{-2}$.
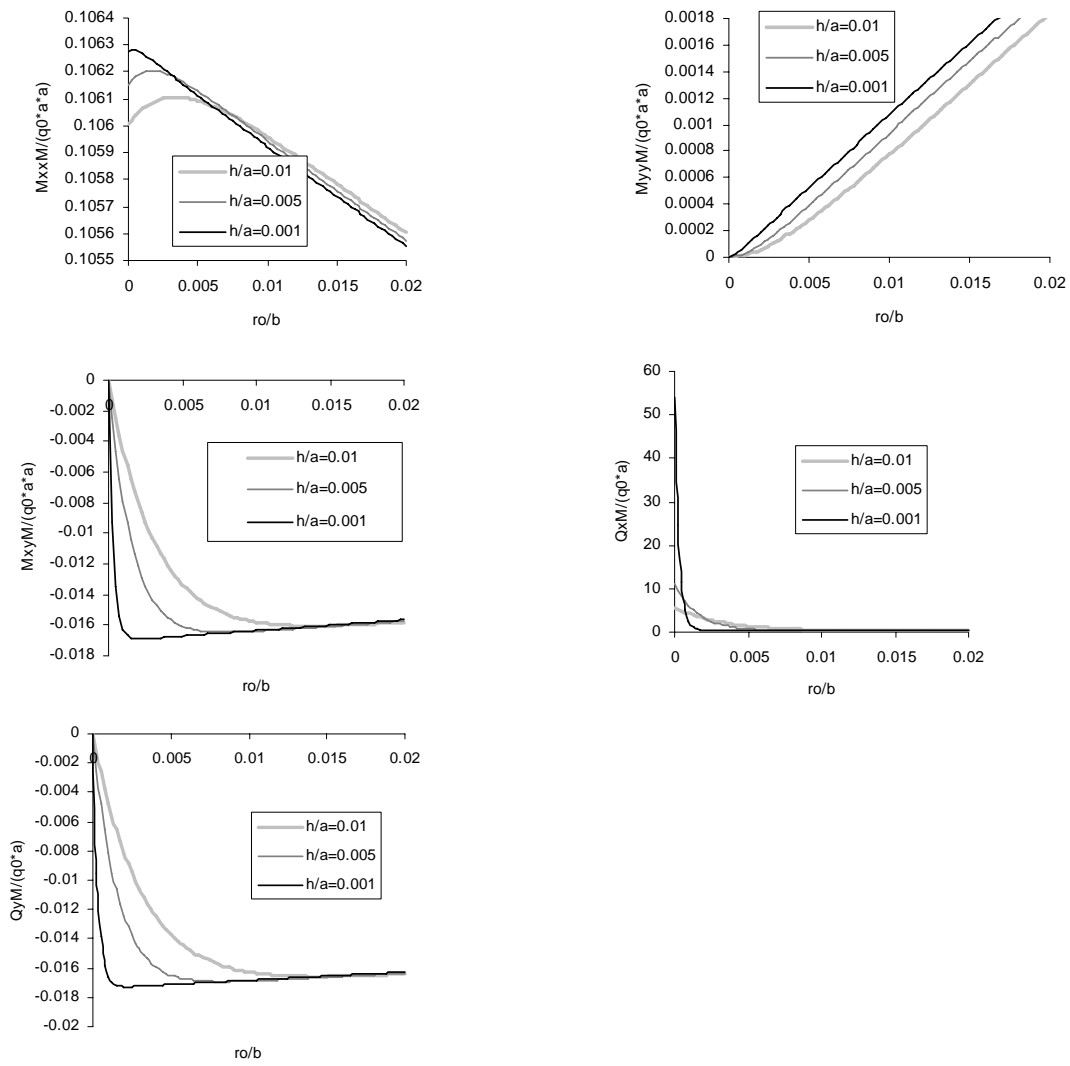
Figure 3. Sqare SH-F plate. Normalized values near the edge $y = b/2$: (a) M_{xx}^{M} at $x=a/2$, (b) M_{yy}^{M} at $x=a/2$, (c) M_{xy}^{M} at $x=a/10$, (d) Q_{x}^{M} at $x=a/10$, (e) Q_{y}^{M} at $x=a/10$.
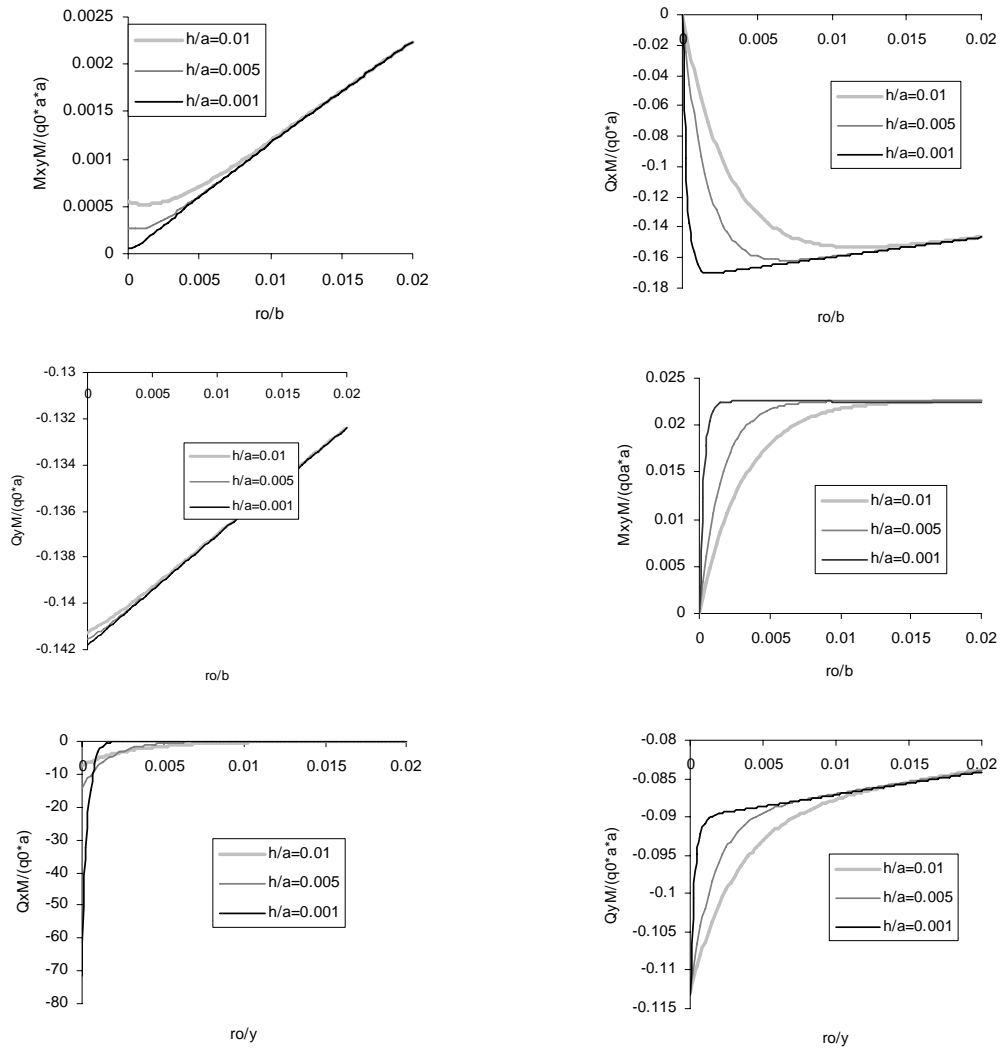
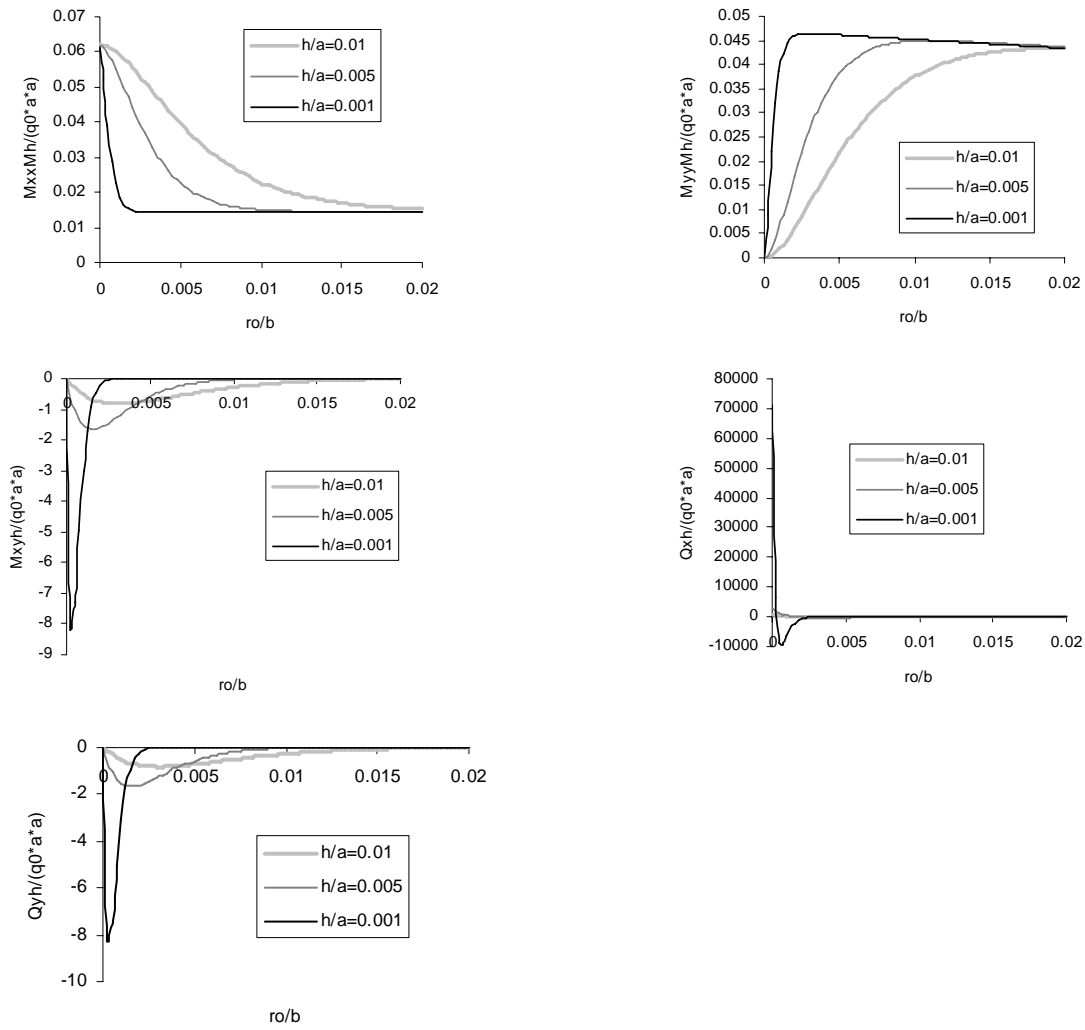Figure 4: Sqare SH-CH plate: Normalized values near the edge $y = b/2$: (a) M_{xy}^M at $x=a/10$, (b) Q_x^M at $x=a/10$, (c) Q_y^M at $x=a/10$. Sqare HS-SS plate: Normalized values near the edge $y = b/2$: (d) M_{xy}^M at $x=a/10$, (e) Q_x^M at $x=a/10$, (f) Q_y^M at $x=a/10$.

Figure 5. Sqare SH-SS plate. Sensitivity of stress resultants on plate thickness. Normalized values near the edge $y = b\,/\,2$: (a) M_{xx}^{M} at $x= a/2$, (b) M_{yy}^{M} at $x=a/2$, (c) M_{xy}^{M} at $x=a/10$, (d) Q_{x}^{M} at $x=a/10$, (e) Q_{y}^{M} at $x=a/10$.
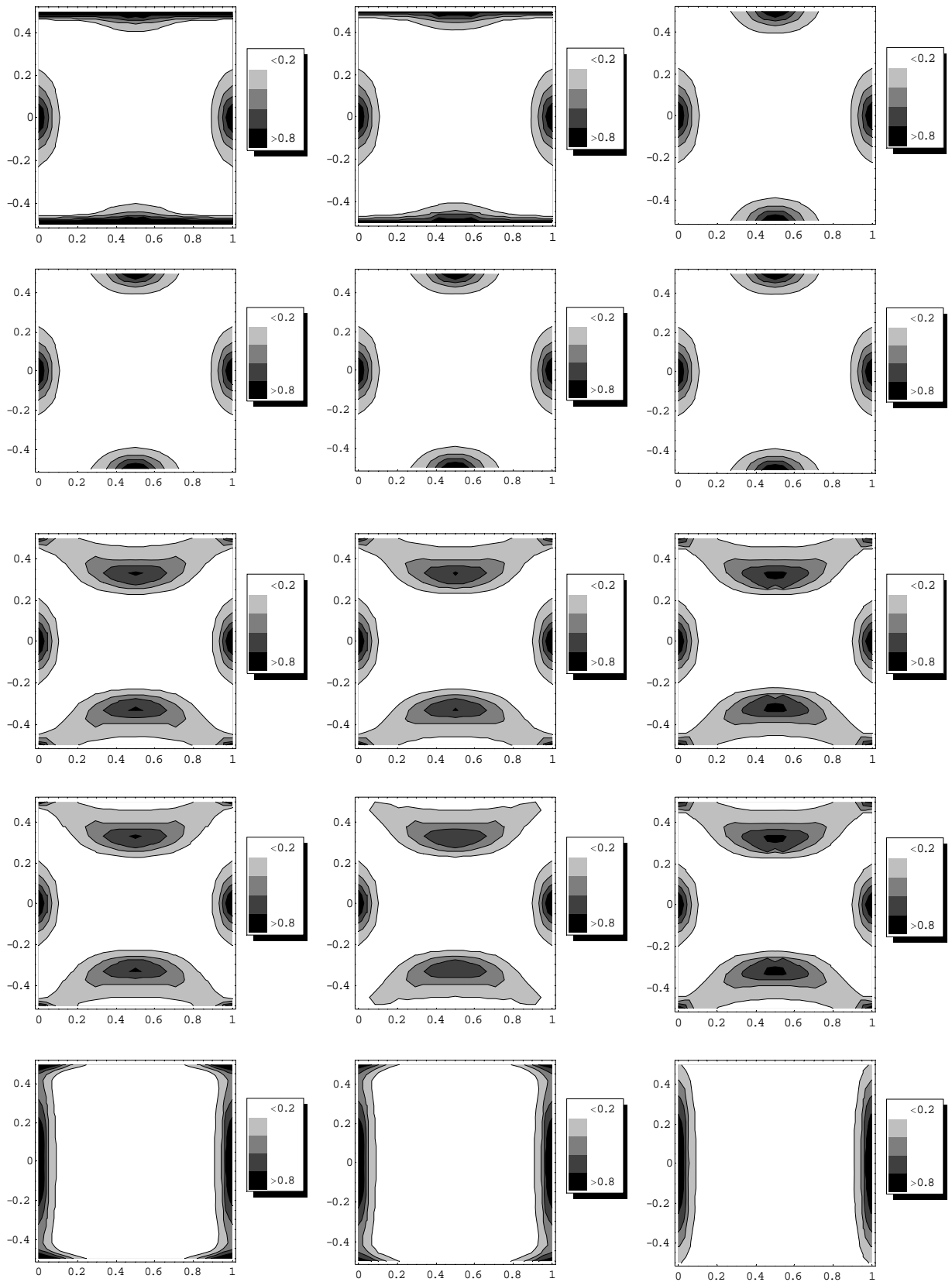
Figure 6. Contour plot of model error for SH-SS plate (first row), SH-SH plate (second row), SH-CS plate (third row), SH-CH plate (fourth row) and SH-F plate (fifth row). Three different model error indicators are used: eq. (28) (first column), eq. (31) (second column) and eq. (33) (third column).
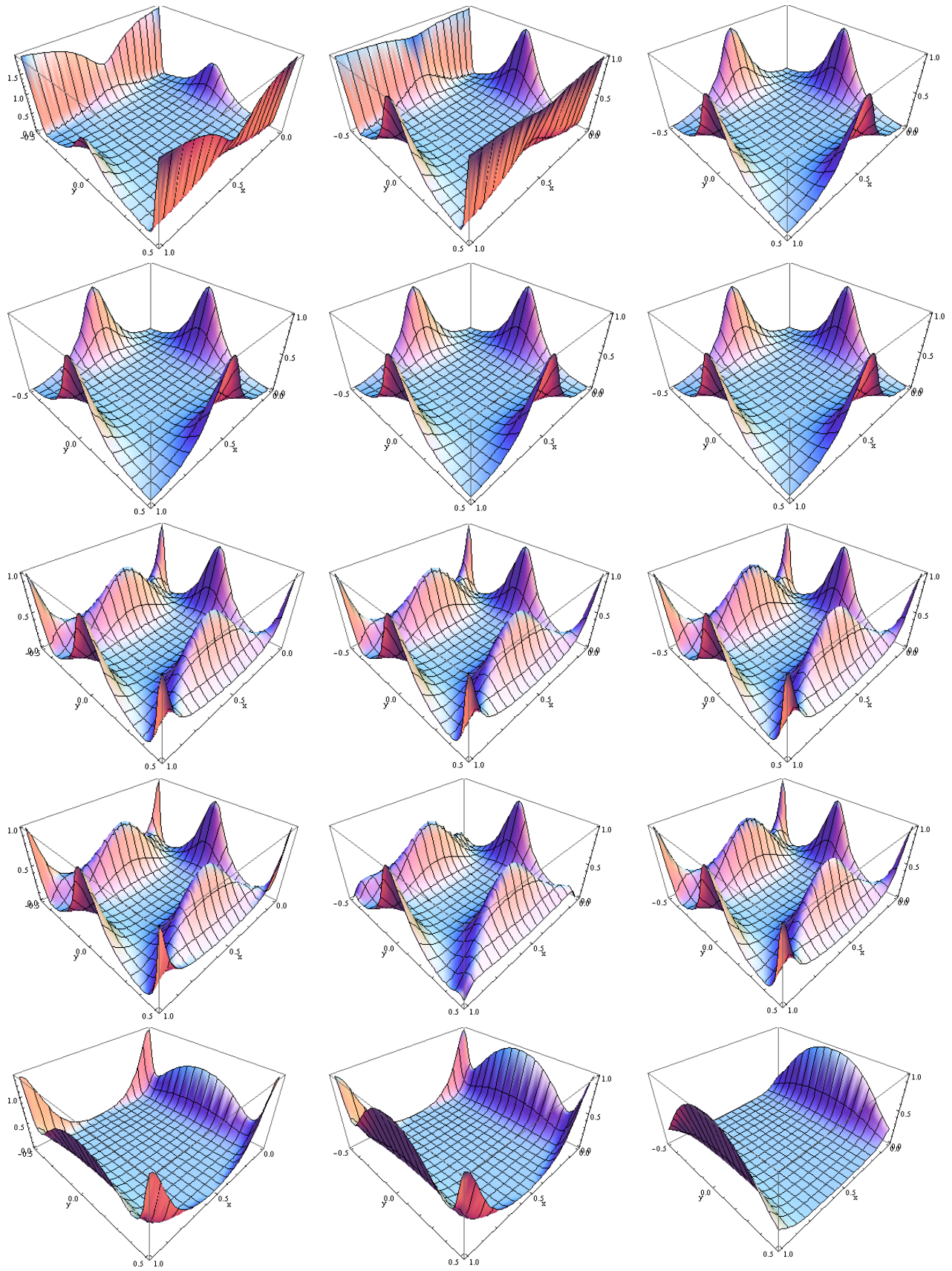
Figure 7. 3d plot of model error for SH-SS plate (first row), SH-SH plate (second row), SH-CS plate (third row), SH-CH plate (fourth row) and SH-F plate (fifth row). Three different model error indicators are used: eq. (28) (first column), eq. (31) (second column) and eq. (33) (third column).
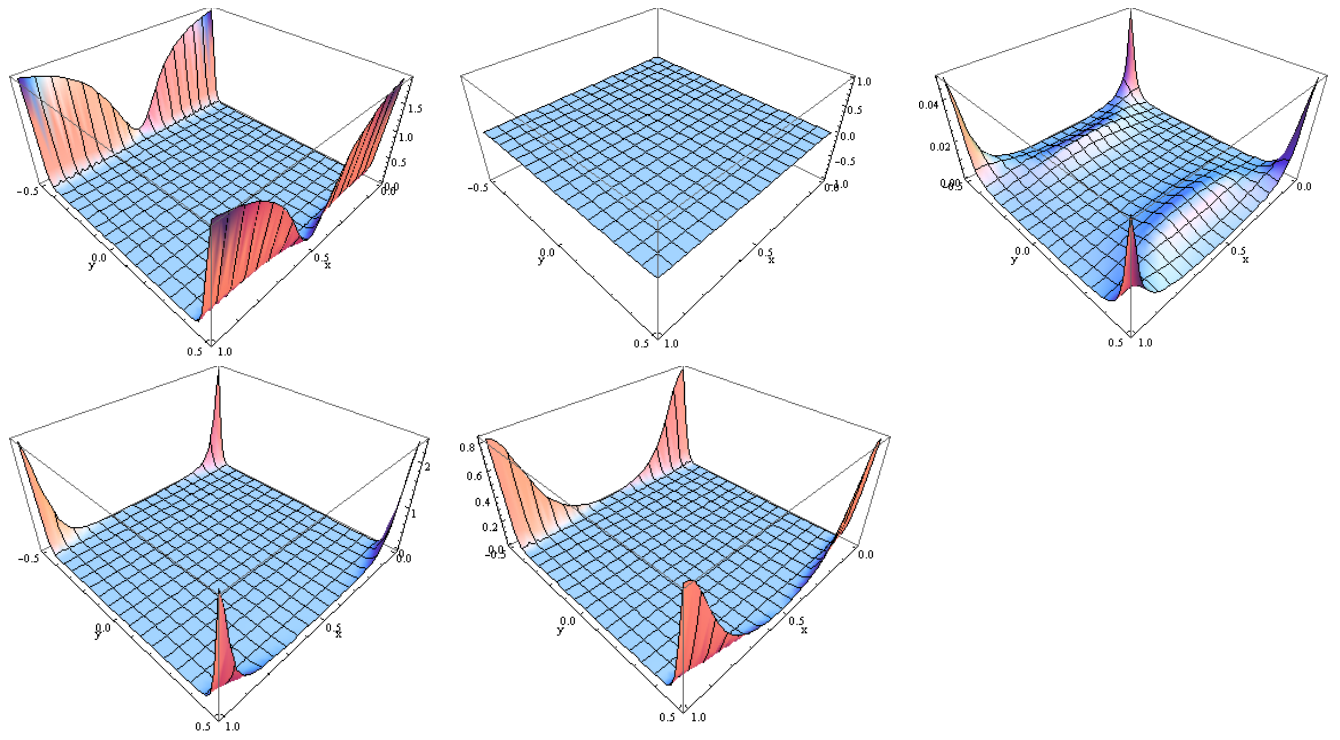
Figure 8. 3d plot of model error (30) for SH-SS, SH-SH and SH-CS plates (first row), and SH-CH and SH-F plates (second row).